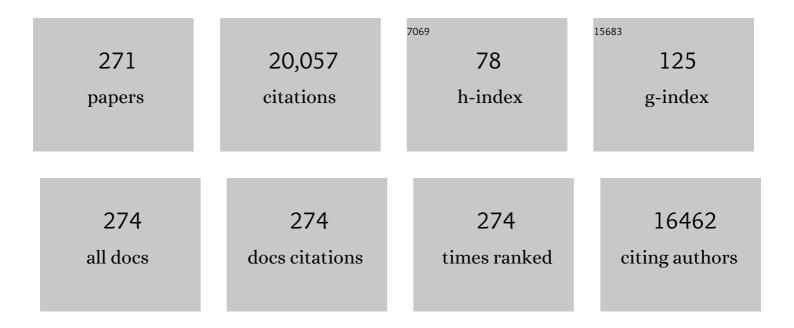
Christian Cambillau

List of Publications by Year in descending order

Source: https://exaly.com/author-pdf/240228/publications.pdf Version: 2024-02-01



#	Article	IF	CITATIONS
1	Protein production and purification. Nature Methods, 2008, 5, 135-146.	9.0	763
2	Interfacial activation of the lipase–procolipase complex by mixed micelles revealed by X-ray crystallography. Nature, 1993, 362, 814-820.	13.7	712
3	Discovery of an RNA virus 3'->5' exoribonuclease that is critically involved in coronavirus RNA synthesis. Proceedings of the National Academy of Sciences of the United States of America, 2006, 103, 5108-5113.	3.3	524
4	Fusarium solani cutinase is a lipolytic enzyme with a catalytic serine accessible to solvent. Nature, 1992, 356, 615-618.	13.7	414
5	Structure of the pancreatic lipase–procolipase complex. Nature, 1992, 359, 159-162.	13.7	374
6	The 2.46 .ANG. Resolution Structure of the Pancreatic Lipase-Colipase Complex Inhibited by a C11 Alkyl Phosphonate. Biochemistry, 1995, 34, 2751-2762.	1.2	286
7	Recognition of antigens by single-domain antibody fragments: the superfluous luxury of paired domains. Trends in Biochemical Sciences, 2001, 26, 230-235.	3.7	283
8	A novel type of catalytic copper cluster in nitrous oxide reductase. Nature Structural Biology, 2000, 7, 191-195.	9.7	280
9	Structural aspects of sexual attraction and chemical communication in insects. Trends in Biochemical Sciences, 2004, 29, 257-264.	3.7	269
10	The severe acute respiratory syndrome-coronavirus replicative protein nsp9 is a single-stranded RNA-binding subunit unique in the RNA virus world. Proceedings of the National Academy of Sciences of the United States of America, 2004, 101, 3792-3796.	3.3	254
11	Structural and Genomic Correlates of Hyperthermostability. Journal of Biological Chemistry, 2000, 275, 32383-32386.	1.6	246
12	Architecture and assembly of the Type VI secretion system. Biochimica Et Biophysica Acta - Molecular Cell Research, 2014, 1843, 1664-1673.	1.9	246
13	Biogenesis and structure of a type VI secretion membrane core complex. Nature, 2015, 523, 555-560.	13.7	241
14	VgrG, Tae, Tle, and beyond: the versatile arsenal of Type VI secretion effectors. Trends in Microbiology, 2014, 22, 498-507.	3.5	240
15	A Common Evolutionary Origin for Tailed-Bacteriophage Functional Modules and Bacterial Machineries. Microbiology and Molecular Biology Reviews, 2011, 75, 423-433.	2.9	234
16	ProteomeBinders: planning a European resource of affinity reagents for analysis of the human proteome. Nature Methods, 2007, 4, 13-17.	9.0	231
17	Revisiting the Specificity of Mamestra brassicaeand Antheraea polyphemus Pheromone-binding Proteins with a Fluorescence Binding Assay. Journal of Biological Chemistry, 2001, 276, 20078-20084.	1.6	217
18	Atomic resolution (1.0 Ã) crystal structure of Fusarium solani cutinase: stereochemical analysis. Journal of Molecular Biology, 1997, 268, 779-799.	2.0	211

#	Article	IF	CITATIONS
19	Structural and Functional Basis for ADP-Ribose and Poly(ADP-Ribose) Binding by Viral Macro Domains. Journal of Virology, 2006, 80, 8493-8502.	1.5	206
20	Domain swapping creates a third putative combining site in bovine odorant binding protein dimer. Nature Structural and Molecular Biology, 1996, 3, 863-867.	3.6	194
21	Structural biology of type VI secretion systems. Philosophical Transactions of the Royal Society B: Biological Sciences, 2012, 367, 1102-1111.	1.8	191
22	A phospholipase A ₁ antibacterial Type VI secretion effector interacts directly with the Câ€ŧerminal domain of the VgrG spike protein for delivery. Molecular Microbiology, 2016, 99, 1099-1118.	1.2	179
23	Cutinase, a lipolytic enzyme with a preformed oxyanion hole. Biochemistry, 1994, 33, 83-89.	1.2	176
24	X-ray Structure and Ligand Binding Study of a Moth Chemosensory Protein. Journal of Biological Chemistry, 2002, 277, 32094-32098.	1.6	173
25	Revisiting the Catalytic CuZ Cluster of Nitrous Oxide (N2O) Reductase. Journal of Biological Chemistry, 2000, 275, 41133-41136.	1.6	166
26	Crystal structure and mechanistic determinants of SARS coronavirus nonstructural protein 15 define an endoribonuclease family. Proceedings of the National Academy of Sciences of the United States of America, 2006, 103, 11892-11897.	3.3	161
27	Directed in Vitro Evolution and Crystallographic Analysis of a Peptide-binding Single Chain Antibody Fragment (scFv) with Low Picomolar Affinity. Journal of Biological Chemistry, 2004, 279, 18870-18877.	1.6	160
28	Moth chemosensory protein exhibits drastic conformational changes and cooperativity on ligand binding. Proceedings of the National Academy of Sciences of the United States of America, 2003, 100, 5069-5074.	3.3	157
29	Ligands for Pheromone-Sensing Neurons Are Not Conformationally Activated Odorant Binding Proteins. PLoS Biology, 2013, 11, e1001546.	2.6	151
30	Crystal Structure of Human Gastric Lipase and Model of Lysosomal Acid Lipase, Two Lipolytic Enzymes of Medical Interest. Journal of Biological Chemistry, 1999, 274, 16995-17002.	1.6	150
31	Widespread anti-CRISPR proteins in virulent bacteriophages inhibit a range of Cas9 proteins. Nature Communications, 2018, 9, 2919.	5.8	147
32	Three Camelid VHH Domains in Complex with Porcine Pancreatic α-Amylase. Journal of Biological Chemistry, 2002, 277, 23645-23650.	1.6	145
33	Camelid Heavy-Chain Variable Domains Provide Efficient Combining Sites to Haptensâ€. Biochemistry, 2000, 39, 1217-1222.	1.2	144
34	Crystal Structure of the Measles Virus Phosphoprotein Domain Responsible for the Induced Folding of the C-terminal Domain of the Nucleoprotein. Journal of Biological Chemistry, 2003, 278, 44567-44573.	1.6	143
35	Structure of lactococcal phage p2 baseplate and its mechanism of activation. Proceedings of the National Academy of Sciences of the United States of America, 2010, 107, 6852-6857.	3.3	143
36	N-terminal arm exchange is observed in the 2.15 Ã crystal structure of oxidized nitrite reductase from Pseudomonas aeruginosa. Structure, 1997, 5, 1157-1171.	1.6	142

#	Article	IF	CITATIONS
37	Complexes of porcine odorant binding protein with odorant molecules belonging to different chemical classes. Journal of Molecular Biology, 2000, 300, 127-139.	2.0	139
38	Crystal structure of Apis mellifera OBP14, a C-minus odorant-binding protein, and its complexes with odorant molecules. Insect Biochemistry and Molecular Biology, 2012, 42, 41-50.	1.2	135
39	High-throughput automated refolding screening of inclusion bodies. Protein Science, 2009, 13, 2782-2792.	3.1	134
40	TOM: a FRODO subpackage for protein-ligand fitting with interactive energy minimization. Journal of Molecular Graphics, 1987, 5, 174-177.	1.7	133
41	Towards a Structural Comprehension of Bacterial Type VI Secretion Systems: Characterization of the TssJ-TssM Complex of an Escherichia coli Pathovar. PLoS Pathogens, 2011, 7, e1002386.	2.1	132
42	The crystal structure of a llama heavy chain variable domain. Nature Structural and Molecular Biology, 1996, 3, 752-757.	3.6	131
43	Priming and polymerization of a bacterial contractile tail structure. Nature, 2016, 531, 59-63.	13.7	127
44	The Structure of the Monomeric Porcine Odorant Binding Protein Sheds Light on the Domain Swapping Mechanism‡. Biochemistry, 1998, 37, 7913-7918.	1.2	126
45	LppX is a lipoprotein required for the translocation of phthiocerol dimycocerosates to the surface of Mycobacterium tuberculosis. EMBO Journal, 2006, 25, 1436-1444.	3.5	126
46	Crystal Structure of Pig Pancreatic alpha-amylase Isoenzyme II, in Complex with the Carbohydrate Inhibitor Acarbose. FEBS Journal, 1996, 238, 561-569.	0.2	125
47	Three-Dimensionnal structures of complexes ofLathyrus ochrus isolectin I with glucose and mannose: Fine specificity of the monosaccharide-binding site. Proteins: Structure, Function and Bioinformatics, 1990, 8, 365-376.	1.5	121
48	Structure of the phage TP901-1 1.8ÂMDa baseplate suggests an alternative host adhesion mechanism. Proceedings of the National Academy of Sciences of the United States of America, 2012, 109, 8954-8958.	3.3	121
49	Lactococcal bacteriophage p2 receptor-binding protein structure suggests a common ancestor gene with bacterial and mammalian viruses. Nature Structural and Molecular Biology, 2006, 13, 85-89.	3.6	117
50	Medium-Scale Structural Genomics:  Strategies for Protein Expression and Crystallization. Accounts of Chemical Research, 2003, 36, 165-172.	7.6	116
51	Receptor-Binding Protein of Lactococcus lactis Phages: Identification and Characterization of the Saccharide Receptor-Binding Site. Journal of Bacteriology, 2006, 188, 2400-2410.	1.0	116
52	The Crystal Structure of a Cockroach Pheromone-binding Protein Suggests a New Ligand Binding and Release Mechanism. Journal of Biological Chemistry, 2003, 278, 30213-30218.	1.6	115
53	Isolation of Llama Antibody Fragments for Prevention of Dandruff by Phage Display in Shampoo. Applied and Environmental Microbiology, 2005, 71, 442-450.	1.4	113
54	Structural genomics on membrane proteins: comparison of more than 100 GPCRs in 3 expression systems. Journal of Structural and Functional Genomics, 2007, 7, 77-91.	1.2	111

#	Article	IF	CITATIONS
55	A Toxin-Antitoxin Module of Salmonella Promotes Virulence in Mice. PLoS Pathogens, 2013, 9, e1003827.	2.1	111
56	Crystal Structure of the Open Form of Dog Gastric Lipase in Complex with a Phosphonate Inhibitor. Journal of Biological Chemistry, 2002, 277, 2266-2274.	1.6	107
57	Horse Pancreatic Lipase. Journal of Molecular Biology, 1994, 238, 709-732.	2.0	106
58	Structures of a legume lectin complexed with the human lactotransferrin N2 fragment, and with an isolated biantennary glycopeptide: role of the fucose moiety. Structure, 1994, 2, 209-219.	1.6	105
59	A pancreatic lipase with a phospholipase A1 activity: crystal structure of a chimeric pancreatic lipase-related protein 2 from guinea pig. Structure, 1996, 4, 1363-1374.	1.6	105
60	Structure-activity of cutinase, a small lipolytic enzyme. Biochimica Et Biophysica Acta - Molecular and Cell Biology of Lipids, 1999, 1441, 185-196.	1.2	104
61	Digestive lipases: From three-dimensional structure to physiology. Biochimie, 2000, 82, 973-986.	1.3	104
62	Modular Structure of the Receptor Binding Proteins of Lactococcus lactis Phages. Journal of Biological Chemistry, 2006, 281, 14256-14262.	1.6	102
63	Camelid nanobodies: killing two birds with one stone. Current Opinion in Structural Biology, 2015, 32, 1-8.	2.6	101
64	TssK Is a Trimeric Cytoplasmic Protein Interacting with Components of Both Phage-like and Membrane Anchoring Complexes of the Type VI Secretion System. Journal of Biological Chemistry, 2013, 288, 27031-27041.	1.6	100
65	Investigation of the Relationship between Lactococcal Host Cell Wall Polysaccharide Genotype and 936 Phage Receptor Binding Protein Phylogeny. Applied and Environmental Microbiology, 2013, 79, 4385-4392.	1.4	99
66	Sulfur Single-wavelength Anomalous Diffraction Crystal Structure of a Pheromone-Binding Protein from the Honeybee Apis mellifera L. Journal of Biological Chemistry, 2004, 279, 4459-4464.	1.6	98
67	Differences in Lactococcal Cell Wall Polysaccharide Structure Are Major Determining Factors in Bacteriophage Sensitivity. MBio, 2014, 5, e00880-14.	1.8	98
68	Contribution of Cutinase Serine 42 Side Chain to the Stabilization of the Oxyanion Transition Stateâ€,â€j. Biochemistry, 1996, 35, 398-410.	1.2	94
69	X-ray crystal structure determination and refinement at 1.9 Ã resolution of isolectin I from the seeds of Lathyrus ochrus. Journal of Molecular Biology, 1990, 214, 571-584.	2.0	92
70	Crystal Structure of E.coli Alcohol Dehydrogenase YqhD: Evidence of a Covalently Modified NADP Coenzyme. Journal of Molecular Biology, 2004, 342, 489-502.	2.0	92
71	Deciphering the Xcp Pseudomonas aeruginosa Type II Secretion Machinery through Multiple Interactions with Substrates. Journal of Biological Chemistry, 2011, 286, 40792-40801.	1.6	91
72	Structural Characterization and Oligomerization of the TssL Protein, a Component Shared by Bacterial Type VI and Type IVb Secretion Systems. Journal of Biological Chemistry, 2012, 287, 14157-14168.	1.6	91

#	Article	IF	CITATIONS
73	ANISEED 2017: extending the integrated ascidian database to the exploration and evolutionary comparison of genome-scale datasets. Nucleic Acids Research, 2018, 46, D718-D725.	6.5	90
74	Pancreatic Lipase Structureâ ´`Function Relationships by Domain Exchange. Biochemistry, 1997, 36, 239-248.	1.2	89
75	Conformational Changes Occurring upon Reduction and NO Binding in Nitrite Reductase fromPseudomonas aeruginosaâ€,‡. Biochemistry, 1998, 37, 13987-13996.	1.2	88
76	Structural Basis of the Honey Bee PBP Pheromone and pH-induced Conformational Change. Journal of Molecular Biology, 2008, 380, 158-169.	2.0	87
77	Reverse chemical ecology: Olfactory proteins from the giant panda and their interactions with putative pheromones and bamboo volatiles. Proceedings of the National Academy of Sciences of the United States of America, 2017, 114, E9802-E9810.	3.3	86
78	Lateral recognition of a dye hapten by a llama VHH domain. Journal of Molecular Biology, 2001, 311, 123-129.	2.0	85
79	Structure, Adsorption to Host, and Infection Mechanism of Virulent Lactococcal Phage p2. Journal of Virology, 2013, 87, 12302-12312.	1.5	85
80	The Insect Attractant 1-Octen-3-ol Is the Natural Ligand of Bovine Odorant-binding Protein. Journal of Biological Chemistry, 2001, 276, 7150-7155.	1.6	80
81	Direct in Vivo Screening of Intrabody Libraries Constructed on a Highly Stable Single-chain Framework. Journal of Biological Chemistry, 2002, 277, 45075-45085.	1.6	80
82	High-throughput protein expression screening and purification in Escherichia coli. Methods, 2011, 55, 65-72.	1.9	80
83	Solution conformation of human neuropeptide Y by 1H nuclear magnetic resonance and restrained molecular dynamics. FEBS Journal, 1992, 209, 765-771.	0.2	79
84	CRYStallize: A crystallographic symmetry display and handling subpackage in TOM/FRODO. Journal of Molecular Graphics, 1990, 8, 86-88.	1.7	78
85	Towards a complete structural deciphering of Type VI secretion system. Current Opinion in Structural Biology, 2018, 49, 77-84.	2.6	78
86	Crystal structure of cutinase covalently inhibited by a triglyceride analogue. Protein Science, 1997, 6, 275-286.	3.1	77
87	Structure and Activity of Rat Pancreatic Lipase-related Protein 2. Journal of Biological Chemistry, 1998, 273, 32121-32128.	1.6	76
88	The Crystal Structure of Odorant Binding Protein 7 from Anopheles gambiae Exhibits an Outstanding Adaptability of Its Binding Site. Journal of Molecular Biology, 2011, 414, 401-412.	2.0	76
89	Functional and structural dissection of the tape measure protein of lactococcal phage TP901-1. Scientific Reports, 2016, 6, 36667.	1.6	75
90	A medium-throughput crystallization approach. Acta Crystallographica Section D: Biological Crystallography, 2002, 58, 2109-2115.	2.5	73

#	Article	IF	CITATIONS
91	Crystal Structure of Bacteriophage SPP1 Distal Tail Protein (gp19.1). Journal of Biological Chemistry, 2010, 285, 36666-36673.	1.6	70
92	Induced refolding of a temperature denatured llama heavy-chain antibody fragment by its antigen. Proteins: Structure, Function and Bioinformatics, 2005, 59, 555-564.	1.5	67
93	Crystal Structure and Kinetics Identify Escherichia coli YdcW Gene Product as a Medium-chain Aldehyde Dehydrogenase. Journal of Molecular Biology, 2004, 343, 29-41.	2.0	66
94	Automated expression and solubility screening of His-tagged proteins in 96-well format. Analytical Biochemistry, 2005, 346, 77-84.	1.1	65
95	Camelid Ig V genes reveal significant human homology not seen in therapeutic target genes, providing for a powerful therapeutic antibody platform. MAbs, 2015, 7, 693-706.	2.6	65
96	Structures and host-adhesion mechanisms of lactococcal siphophages. Frontiers in Microbiology, 2014, 5, 3.	1.5	63
97	Preanalytical Issues and Cycle Threshold Values in SARS-CoV-2 Real-Time RT-PCR Testing: Should Test Results Include These?. ACS Omega, 2021, 6, 6528-6536.	1.6	63
98	Crystal structure of a ternary complex between human chorionic gonadotropin (hCG) and two Fv fragments specific for the α and β-subunits 1 1Edited by I. A. Wilson. Journal of Molecular Biology, 1999, 289, 1375-1385.	2.0	62
99	Crystal Structure of the Receptor-Binding Protein Head Domain from Lactococcus lactis Phage blL170. Journal of Virology, 2006, 80, 9331-9335.	1.5	62
100	Queen Bee Pheromone Binding Protein pH-Induced Domain Swapping Favors Pheromone Release. Journal of Molecular Biology, 2009, 390, 981-990.	2.0	62
101	Expression and characterization of the protein Rv1399c from Mycobacterium tuberculosis. FEBS Journal, 2004, 271, 3953-3961.	0.2	61
102	An essential role for the baseplate protein Gp45 in phage adsorption to Staphylococcus aureus. Scientific Reports, 2016, 6, 26455.	1.6	61
103	Crystal Structure of the VgrG1 Actin Cross-linking Domain of the Vibrio cholerae Type VI Secretion System. Journal of Biological Chemistry, 2012, 287, 38190-38199.	1.6	60
104	Characterization of the Porphyromonas gingivalis Type IX Secretion Trans-envelope PorKLMNP Core Complex. Journal of Biological Chemistry, 2017, 292, 3252-3261.	1.6	60
105	Crystal structure of a cohesin module from Clostridium cellulolyticum: implications for dockerin recognition. Journal of Molecular Biology, 2000, 304, 189-200.	2.0	59
106	Crystallographic study of the structure of colipase and of the interaction with pancreatic lipase. Protein Science, 1995, 4, 44-57.	3.1	58
107	Complexation of Two Proteic Insect Inhibitors to the Active Site of Chymotrypsin Suggests Decoupled Roles for Binding and Selectivity. Journal of Biological Chemistry, 2001, 276, 38893-38898.	1.6	58
108	The XcpV/GspI Pseudopilin Has a Central Role in the Assembly of a Quaternary Complex within the T2SS Pseudopilus. Journal of Biological Chemistry, 2009, 284, 34580-34589.	1.6	58

#	Article	IF	CITATIONS
109	The Atomic Structure of the Phage Tuc2009 Baseplate Tripod Suggests that Host Recognition Involves Two Different Carbohydrate Binding Modules. MBio, 2016, 7, e01781-15.	1.8	58
110	Dynamics ofFusarium solani cutinase investigated through structural comparison among different crystal forms of its variants. Proteins: Structure, Function and Bioinformatics, 1996, 26, 442-458.	1.5	57
111	Structure and activity of <scp>AbiQ</scp> , a lactococcal endoribonuclease belonging to the type <scp>III</scp> toxin–antitoxin system. Molecular Microbiology, 2013, 87, 756-768.	1.2	57
112	Bivalent Llama Single-Domain Antibody Fragments against Tumor Necrosis Factor Have Picomolar Potencies due to Intramolecular Interactions. Frontiers in Immunology, 2017, 8, 867.	2.2	57
113	The Importance of Framework Residues H6, H7 and H10 in Antibody Heavy Chains: Experimental Evidence for a New Structural Subclassification of Antibody VH Domains. Journal of Molecular Biology, 2001, 309, 701-716.	2.0	55
114	Crystal Structure and Function of a DARPin Neutralizing Inhibitor of Lactococcal Phage TP901-1. Journal of Biological Chemistry, 2009, 284, 30718-30726.	1.6	55
115	Structure and Molecular Assignment of Lactococcal Phage TP901-1 Baseplate. Journal of Biological Chemistry, 2010, 285, 39079-39086.	1.6	55
116	Visualizing a Complete Siphoviridae Member by Single-Particle Electron Microscopy: the Structure of Lactococcal Phage TP901-1. Journal of Virology, 2013, 87, 1061-1068.	1.5	55
117	Type IX secretion system PorM and gliding machinery GldM form arches spanning the periplasmic space. Nature Communications, 2018, 9, 429.	5.8	54
118	Molecular Insights on the Recognition of a Lactococcus lactis Cell Wall Pellicle by the Phage 1358 Receptor Binding Protein. Journal of Virology, 2014, 88, 7005-7015.	1.5	53
119	Boar salivary lipocalin. FEBS Journal, 2002, 269, 2449-2456.	0.2	52
120	Crystal structure of a novel type of odorant-binding protein from <i>Anopheles gambiae</i> , belonging to the C-plus class. Biochemical Journal, 2011, 437, 423-430.	1.7	52
121	Crystal structures of bovine odorant-binding protein in complex with odorant molecules. FEBS Journal, 2004, 271, 3832-3842.	0.2	51
122	A Topological Model of the Baseplate of Lactococcal Phage Tuc2009. Journal of Biological Chemistry, 2008, 283, 2716-2723.	1.6	51
123	Crystal structure of the DNA-bound VapBC2 antitoxin/toxin pair from Rickettsia felis. Nucleic Acids Research, 2012, 40, 3245-3258.	6.5	51
124	Effect of Rickettsial Toxin VapC on Its Eukaryotic Host. PLoS ONE, 2011, 6, e26528.	1.1	51
125	Control of domain swapping in bovine odorant-binding protein. Biochemical Journal, 2002, 365, 739-748.	1.7	50
126	From The Cover: An aminoacyl-tRNA synthetase-like protein encoded by the Escherichia coli yadB gene glutamylates specifically tRNAAsp. Proceedings of the National Academy of Sciences of the United States of America, 2004, 101, 7530-7535.	3.3	50

#	Article	IF	CITATIONS
127	Plant stress proteins of the thaumatin-like family discovered in animals. FEBS Letters, 2004, 572, 3-7.	1.3	49
128	The membrane bound bacterial lipocalin Blc is a functional dimer with binding preference for lysophospholipids. FEBS Letters, 2006, 580, 4877-4883.	1.3	48
129	Type VI secretion TssK baseplate protein exhibits structural similarity with phage receptor-binding proteins and evolved to bind the membrane complex. Nature Microbiology, 2017, 2, 17103.	5.9	48
130	A Cutinase from Trichoderma reesei with a Lid-Covered Active Site and Kinetic Properties of True Lipases. Journal of Molecular Biology, 2014, 426, 3757-3772.	2.0	47
131	The gp27-like Hub of VgrG Serves as Adaptor to Promote Hcp Tube Assembly. Journal of Molecular Biology, 2018, 430, 3143-3156.	2.0	47
132	Crystal structure of aphrodisin, a sex pheromone from female hamster11Edited by R Huber. Journal of Molecular Biology, 2001, 305, 459-469.	2.0	46
133	Structure and Functional Analysis of the Host Recognition Device of Lactococcal Phage Tuc2009. Journal of Virology, 2013, 87, 8429-8440.	1.5	46
134	A pheromone-binding protein from the cockroach Leucophaea maderae: cloning, expression and pheromone binding. Biochemical Journal, 2003, 371, 573-579.	1.7	45
135	The Escherichia coli YadB Gene Product Reveals a Novel Aminoacyl-tRNA Synthetase Like Activity. Journal of Molecular Biology, 2004, 337, 273-283.	2.0	45
136	The crystal structure of the Escherichia coli lipocalin Blc suggests a possible role in phospholipid binding. FEBS Letters, 2004, 562, 183-188.	1.3	45
137	VaZyMolO: a tool to define and classify modularity in viral proteins. Journal of General Virology, 2005, 86, 743-749.	1.3	45
138	Mammalian G protein-coupled receptor expression in Escherichia coli: II. Refolding and biophysical characterization of mouse cannabinoid receptor 1 and human parathyroid hormone receptor 1. Analytical Biochemistry, 2010, 401, 74-80.	1.1	45
139	Viral infection modulation and neutralization by camelid nanobodies. Proceedings of the National Academy of Sciences of the United States of America, 2013, 110, E1371-9.	3.3	45
140	Cas9 Allosteric Inhibition by the Anti-CRISPR Protein AcrIIA6. Molecular Cell, 2019, 76, 922-937.e7.	4.5	44
141	Crystal Structure and Self-Interaction of the Type VI Secretion Tail-Tube Protein from Enteroaggregative Escherichia coli. PLoS ONE, 2014, 9, e86918.	1.1	44
142	Solution structure of human corticotropin releasing factor by 1H NMR and distance geometry with restrained molecular dynamics. Protein Engineering, Design and Selection, 1993, 6, 149-156.	1.0	43
143	A Hyperthermostable D-Ribose-5-Phosphate Isomerase from Pyrococcus horikoshii Characterization and Three-Dimensional Structure. Structure, 2002, 10, 877-886.	1.6	43
144	A minimalist glutamyl-tRNA synthetase dedicated to aminoacylation of the tRNAAsp QUC anticodon. Nucleic Acids Research, 2004, 32, 2768-2775.	6.5	43

#	Article	IF	CITATIONS
145	<scp>X</scp> â€ray structure of a superinfection exclusion lipoprotein from phage <scp>TP</scp> â€ <scp>J</scp> 34 and identification of the tape measure protein as its target. Molecular Microbiology, 2013, 89, 152-165.	1.2	43
146	Structure of the host-recognition device of Staphylococcus aureus phage ϕ11. Scientific Reports, 2016, 6, 27581.	1.6	42
147	Recombinant pheromone binding protein 1 from Mamestra brassicae (MbraPBP1) . Functional and structural characterization. FEBS Journal, 1999, 264, 707-716.	0.2	41
148	Acidianus filamentous virus 1 coat proteins display a helical fold spanning the filamentous archaeal viruses lineage. Proceedings of the National Academy of Sciences of the United States of America, 2009, 106, 21155-21160.	3.3	41
149	There is a baby in the bath water: AcrB contamination is a major problem in membrane-protein crystallization. Acta Crystallographica Section F: Structural Biology Communications, 2008, 64, 880-885.	0.7	40
150	The Opening of the SPP1 Bacteriophage Tail, a Prevalent Mechanism in Gram-positive-infecting Siphophages. Journal of Biological Chemistry, 2011, 286, 25397-25405.	1.6	40
151	Isoform purification of gastric lipases. Journal of Molecular Biology, 1992, 225, 147-153.	2.0	39
152	The targeted recognition of <scp><i>L</i></scp> <i>actococcus lactis</i> phages to their polysaccharide receptors. Molecular Microbiology, 2015, 96, 875-886.	1.2	39
153	Crystallization of Pancreatic Procolipase and of its Complex with Pancreatic Lipase. Journal of Molecular Biology, 1993, 229, 552-554.	2.0	37
154	Getting the best out of long-wavelength X-rays: <i>de novo</i> chlorine/sulfur SAD phasing of a structural protein from ATV. Acta Crystallographica Section D: Biological Crystallography, 2010, 66, 304-308.	2.5	37
155	TssA: The cap protein of the Type VI secretion system tail. BioEssays, 2017, 39, 1600262.	1.2	37
156	Structure of the type VI secretion system TssK–TssF–TssG baseplate subcomplex revealed by cryo-electron microscopy. Nature Communications, 2018, 9, 5385.	5.8	37
157	Selection, Characterization and X-ray Structure of Anti-ampicillin Single-chain Fv Fragments from Phage-displayed Murine Antibody Libraries. Journal of Molecular Biology, 2001, 309, 671-685.	2.0	36
158	Solution and electron microscopy characterization of lactococcal phage baseplates expressed in Escherichia coli. Journal of Structural Biology, 2010, 172, 75-84.	1.3	35
159	The First Structure of a Mycobacteriophage, the Mycobacterium abscessus subsp. bolletii Phage Araucaria. Journal of Virology, 2013, 87, 8099-8109.	1.5	35
160	Evolved distal tail carbohydrate binding modules of <scp><i>L</i></scp> <i>actobacillus</i> phage <scp>J</scp> â€1: a novel type of antiâ€receptor widespread among lactic acid bacteria phages. Molecular Microbiology, 2017, 104, 608-620.	1.2	35
161	Host recognition by lactic acid bacterial phages. FEMS Microbiology Reviews, 2017, 41, S16-S26.	3.9	35
162	Neutralization of Human Interleukin 23 by Multivalent Nanobodies Explained by the Structure of Cytokine–Nanobody Complex. Frontiers in Immunology, 2017, 8, 884.	2.2	35

#	Article	IF	CITATIONS
163	A Decade of Streptococcus thermophilus Phage Evolution in an Irish Dairy Plant. Applied and Environmental Microbiology, 2018, 84, .	1.4	35
164	Molecular cloning and bacterial expression of a general odorant-binding protein from the cabbage armyworm Mamestra brassicae. FEBS Journal, 1998, 258, 768-774.	0.2	34
165	The structure of an entire noncovalent immunoglobulin kappa light-chain dimer (Bence-Jones protein) reveals a weak and unusual constant domains association. FEBS Journal, 1999, 260, 192-199.	0.2	34
166	Structural genomics of the SARS coronavirus: cloning, expression, crystallization and preliminary crystallographic study of the Nsp9 protein. Acta Crystallographica Section D: Biological Crystallography, 2003, 59, 1628-1631.	2.5	34
167	The Crystal Structure of the Escherichia coli YfdW Gene Product Reveals a New Fold of Two Interlaced Rings Identifying a Wide Family of CoA Transferases. Journal of Biological Chemistry, 2003, 278, 34582-34586.	1.6	34
168	Mammalian G-protein-coupled receptor expression in Escherichia coli: I. High-throughput large-scale production as inclusion bodies. Analytical Biochemistry, 2009, 386, 147-155.	1.1	34
169	Conserved and Diverse Traits of Adhesion Devices from Siphoviridae Recognizing Proteinaceous or Saccharidic Receptors. Viruses, 2020, 12, 512.	1.5	34
170	The 2.6â€Ã refined structure of the <i>Escherichia coli</i> recombinant <i>Saccharomyces cerevisiae</i> flavocytochrome <i>b</i> ₂ â€sulfite complex. Protein Science, 1994, 3, 303-313.	3.1	33
171	Solution structure and backbone dynamics of an antigen-free heavy chain variable domain (VHH) fromLlama. Proteins: Structure, Function and Bioinformatics, 2002, 47, 546-555.	1.5	33
172	X-ray and Cryo-electron Microscopy Structures of Monalysin Pore-forming Toxin Reveal Multimerization of the Pro-form. Journal of Biological Chemistry, 2015, 290, 13191-13201.	1.6	33
173	Structure–Function Analysis of the TssL Cytoplasmic Domain Reveals a New Interaction between the Type VI Secretion Baseplate and Membrane Complexes. Journal of Molecular Biology, 2016, 428, 4413-4423.	2.0	33
174	Domain swapping of a llama VHH domain builds a crystal-wide β-sheet structure. FEBS Letters, 2004, 564, 35-40.	1.3	32
175	Functional carbohydrate binding modules identified in evolved dits from siphophages infecting various Gramâ€positive bacteria. Molecular Microbiology, 2018, 110, 777-795.	1.2	32
176	Does the Reduction of c Heme Trigger the Conformational Change of Crystalline Nitrite Reductase?. Journal of Biological Chemistry, 1999, 274, 14997-15004.	1.6	31
177	Glu-Q-tRNAAsp synthetase coded by the yadB gene, a new paralog of aminoacyl-tRNA synthetase that glutamylates tRNAAsp anticodon. Biochimie, 2005, 87, 847-861.	1.3	31
178	Crystal structure of AFV3-109, a highly conserved protein from crenarchaeal viruses. Virology Journal, 2007, 4, 12.	1.4	31
179	Structure and specificity of the Type VI secretion system ClpV-TssC interaction in enteroaggregative Escherichia coli. Scientific Reports, 2016, 6, 34405.	1.6	31
180	Interactions of plant lectins with the components of the bacterial cell wall peptidoglycan. Biochemical Systematics and Ecology, 1994, 22, 153-159.	0.6	30

#	Article	IF	CITATIONS
181	MAD Structure of Pseudomonas nautica Dimeric Cytochrome c552Mimicks thec4 Dihemic Cytochrome Domain Association. Journal of Molecular Biology, 1999, 289, 1017-1028.	2.0	30
182	Cryo-Electron Microscopy Structure of Lactococcal Siphophage 1358 Virion. Journal of Virology, 2014, 88, 8900-8910.	1.5	30
183	Chemosensory protein from the mothMamestra brassicae. FEBS Journal, 2001, 268, 4731-4739.	0.2	29
184	Genetic and functional characterisation of the lactococcal P335 phage-host interactions. BMC Genomics, 2017, 18, 146.	1.2	29
185	Camelid nanobodies raised against an integral membrane enzyme, nitric oxide reductase. Protein Science, 2009, 18, 619-628.	3.1	28
186	Expanding the molecular toolbox for Lactococcus lactis: construction of an inducible thioredoxin gene fusion expression system. Microbial Cell Factories, 2011, 10, 66.	1.9	28
187	Involvement of the Major Capsid Protein and Two Early-Expressed Phage Genes in the Activity of the Lactococcal Abortive Infection Mechanism AbiT. Applied and Environmental Microbiology, 2012, 78, 6890-6899.	1.4	28
188	Crystallization and preliminary X-ray study of horse pancreatic lipase. Journal of Molecular Biology, 1989, 205, 259-261.	2.0	27
189	A mutation designed to alter crystal packing permits structural analysis of a tight-binding fluorescein-scFv complex. Protein Science, 2005, 14, 2537-2549.	3.1	27
190	Crystallization, preliminary X-ray study and crystal activity of the hydrogenase from Desulfovibrio gigas. Journal of Molecular Biology, 1987, 195, 969-971.	2.0	26
191	Engineering cysteine mutants to obtain crystallographic phases with a cutinase from Fusarium solani pisi. Protein Engineering, Design and Selection, 1993, 6, 157-165.	1.0	26
192	Crystal Structure of ORF12 from <i>Lactococcus lactis</i> Phage p2 Identifies a Tape Measure Protein Chaperone. Journal of Bacteriology, 2009, 191, 728-734.	1.0	26
193	A hypothetical complex between crystalline flavocytochromeb2 and Cytochromec. Proteins: Structure, Function and Bioinformatics, 1993, 16, 408-422.	1.5	25
194	Crystal structure of the conserved hypothetical protein Rv1155 fromMycobacterium tuberculosis. FEBS Letters, 2005, 579, 215-221.	1.3	25
195	Amino acid sequence determination and three-dimensional modelling of thioredoxin from the photosynthetic bacterium Rhodobacter sphaeroides Y. FEBS Journal, 1988, 172, 413-419.	0.2	24
196	Unraveling Lactococcal Phage Baseplate Assembly by Mass Spectrometry. Molecular and Cellular Proteomics, 2011, 10, M111.009787.	2.5	24
197	Structural Mimicry of Receptor Interaction by Antagonistic Interleukin-6 (IL-6) Antibodies. Journal of Biological Chemistry, 2016, 291, 13846-13854.	1.6	24
198	The inactive subunit of ruminant procarboxypeptidase A-S6 complexes. Structural basis of inactivity and physiological role. FEBS Journal, 1986, 157, 531-538.	0.2	23

#	Article	IF	CITATIONS
199	Lactococcal Abortive Infection Protein AbiV Interacts Directly with the Phage Protein SaV and Prevents Translation of Phage Proteins. Applied and Environmental Microbiology, 2010, 76, 7085-7092.	1.4	23
200	Lactococcal phage p2 ORF35‧ak3 is an ATPase involved in DNA recombination and AbiK mechanism. Molecular Microbiology, 2011, 80, 102-116.	1.2	23
201	Domain Swing Upon His to Ala Mutation in Nitrite Reductase of Pseudomonas aeruginosa. Journal of Molecular Biology, 2001, 312, 541-554.	2.0	22
202	Differential Substrate Specificity and Kinetic Behavior of <i>Escherichia coli</i> YfdW and <i>Oxalobacter formigenes</i> Formyl Coenzyme A Transferase. Journal of Bacteriology, 2008, 190, 2556-2564.	1.0	22
203	Crystal Structure of a Chimeric Receptor Binding Protein Constructed from Two Lactococcal Phages. Journal of Bacteriology, 2009, 191, 3220-3225.	1.0	22
204	Characterization of prophages containing "evolved―Dit/Tal modules in the genome of Lactobacillus casei BL23. Applied Microbiology and Biotechnology, 2016, 100, 9201-9215.	1.7	22
205	Biochemical and Structural Characterization of TesA, a Major Thioesterase Required for Outer-Envelope Lipid Biosynthesis in Mycobacterium tuberculosis. Journal of Molecular Biology, 2018, 430, 5120-5136.	2.0	22
206	Novel Genus of Phages Infecting Streptococcus thermophilus: Genomic and Morphological Characterization. Applied and Environmental Microbiology, 2020, 86, .	1.4	22
207	Deciphering the function of lactococcal phage ul36 Sak domains. Journal of Structural Biology, 2010, 170, 462-469.	1.3	20
208	Revisiting the host adhesion determinants of <i>Streptococcus thermophilus</i> siphophages. Microbial Biotechnology, 2020, 13, 1765-1779.	2.0	20
209	Crystallization and preliminary X-ray study of a recombinant cutinase from Fusarium solani pisi. Journal of Molecular Biology, 1990, 215, 215-216.	2.0	19
210	Crystallization and Preliminary X-ray Diffraction Studies of the Soluble 14 kDa β-Galactoside-binding Lectin from Bovine Heart. Journal of Molecular Biology, 1994, 235, 787-789.	2.0	19
211	Cyanide Binding to cd1 Nitrite Reductase from Pseudomonas aeruginosa: Role of the Active-Site His369 in Ligand Stabilization. Biochemical and Biophysical Research Communications, 2002, 291, 1-7.	1.0	19
212	Optimization of crystals from nanodrops: crystallization and preliminary crystallographic study of a pheromone-binding protein from the honeybeeApis melliferaL Acta Crystallographica Section D: Biological Crystallography, 2003, 59, 919-921.	2.5	19
213	Quaternary structure of alpha-crustacyanin from lobster as seen by small-angle X-ray scattering. FEBS Letters, 2003, 544, 189-193.	1.3	19
214	Dissection of the TssB-TssC Interface during Type VI Secretion Sheath Complex Formation. PLoS ONE, 2013, 8, e81074.	1.1	19
215	Ubiquitous Carbohydrate Binding Modules Decorate 936 Lactococcal Siphophage Virions. Viruses, 2019, 11, 631.	1.5	19
216	The CWPS Rubik's cube: Linking diversity of cell wall polysaccharide structures with the encoded biosynthetic machinery of selected <i>Lactococcus lactis</i> strains. Molecular Microbiology, 2020, 114, 582-596.	1.2	19

#	Article	IF	CITATIONS
217	Structure and Assembly of TP901-1 Virion Unveiled by Mutagenesis. PLoS ONE, 2015, 10, e0131676.	1.1	19
218	Crystal structure and reactivity of YbdL fromEscherichia coliidentify a methionine aminotransferase function. FEBS Letters, 2004, 571, 141-146.	1.3	18
219	Production and biophysical characterization of the CorA transporter from Methanosarcina mazei. Analytical Biochemistry, 2009, 388, 115-121.	1.1	18
220	Structure and Topology Prediction of Phage Adhesion Devices Using AlphaFold2: The Case of Two Oenococcus oeni Phages. Microorganisms, 2021, 9, 2151.	1.6	18
221	Present Impact of AlphaFold2 Revolution on Structural Biology, and an Illustration With the Structure Prediction of the Bacteriophage J-1 Host Adhesion Device. Frontiers in Molecular Biosciences, 2022, 9, .	1.6	18
222	Construction of two Lactococcus lactis expression vectors combining the Gateway and the NIsin Controlled Expression systems. Plasmid, 2011, 66, 129-135.	0.4	17
223	Camelid nanobodies used as crystallization chaperones for different constructs of PorM, a component of the type IX secretion system from <i>Porphyromonas gingivalis</i> . Acta Crystallographica Section F, Structural Biology Communications, 2017, 73, 286-293.	0.4	17
224	The role of the surface ligand on the performance of electrochemical SARS-CoV-2 antigen biosensors. Analytical and Bioanalytical Chemistry, 2022, 414, 103-113.	1.9	17
225	Inhibition of Type VI Secretion by an Anti-TssM Llama Nanobody. PLoS ONE, 2015, 10, e0122187.	1.1	16
226	Subunit III of ruminant procarboxypeptidase A-S6 complexes and pancreatic proteases E a new family of pancreatic serine endopeptidases?. FEBS Letters, 1988, 232, 91-95.	1.3	15
227	Structure ofEscherichia coliYhdH, a putative quinone oxidoreductase. Acta Crystallographica Section D: Biological Crystallography, 2004, 60, 1855-1862.	2.5	15
228	Structure and function of phage p2 ORF34 _{p2} , a new type of singleâ€stranded DNA binding protein. Molecular Microbiology, 2009, 73, 1156-1170.	1.2	15
229	<i>Lactococcus lactis</i> phage TP901–1 as a model for <i>Siphoviridae</i> virion assembly. Bacteriophage, 2016, 6, e1123795.	1.9	15
230	High-Throughput Protein Production Combined with High- Throughput SELEX Identifies an Extensive Atlas of Ciona robusta Transcription Factor DNA-Binding Specificities. Methods in Molecular Biology, 2019, 2025, 487-517.	0.4	15
231	[5] Pancreatic lipases and their complexes with colipases and inhibitors: Crystallization and crystal packing. Methods in Enzymology, 1997, 284, 107-119.	0.4	14
232	ORF157 from the Archaeal Virus <i>Acidianus</i> Filamentous Virus 1 Defines a New Class of Nuclease. Journal of Virology, 2010, 84, 5025-5031.	1.5	14
233	Crystallization and preliminary X-ray diffraction study of Lathyrus ochrus isolectin II complexed to the human lactotransferrin N2 fragment. Journal of Molecular Biology, 1992, 227, 938-941.	2.0	13
234	The thermo―and acidoâ€stable ORFâ€99 from the archaeal virus AFV1. Protein Science, 2009, 18, 1316-1320.	3.1	13

#	Article	IF	CITATIONS
235	An inactive pancreatic—related protein is activated into a triglyceride-lipase by mutagenesis based on the 3-D structure. Chemistry and Physics of Lipids, 1998, 93, 103-114.	1.5	12
236	Crystal structure of <i>Bacillus subtilis</i> SPP1 phage gp22 shares fold similarity with a domain of lactococcal phage p2 RBP. Protein Science, 2010, 19, 1439-1443.	3.1	12
237	Biochemical and structural characterization of non-glycosylatedYarrowia lipolyticaLIP2 lipase. European Journal of Lipid Science and Technology, 2013, 115, 429-441.	1.0	12
238	Identification of Dual Receptor Binding Protein Systems in Lactococcal 936 Group Phages. Viruses, 2018, 10, 668.	1.5	12
239	Crystal structure of Type IX secretion system PorE C-terminal domain from Porphyromonas gingivalis in complex with a peptidoglycan fragment. Scientific Reports, 2020, 10, 7384.	1.6	12
240	Characterization of the First Virulent Phage Infecting Oenococcus oeni, the Queen of the Cellars. Frontiers in Microbiology, 2020, 11, 596541.	1.5	12
241	Recombinant chemosensory protein (CSP2) from the mothMamestra brassicae: crystallization and preliminary crystallographic study. Acta Crystallographica Section D: Biological Crystallography, 2001, 57, 137-139.	2.5	11
242	Crystal structure of <i>Bacillus subtilis</i> SPP1 phage gp23.1, a putative chaperone. Protein Science, 2010, 19, 1812-1816.	3.1	11
243	Bacteriophage module reshuffling results in adaptive host range as exemplified by the baseplate model of listerial phage A118. Virology, 2015, 484, 86-92.	1.1	11
244	The Baseplate of Lactobacillus delbrueckii Bacteriophage Ld17 Harbors a Glycerophosphodiesterase. Journal of Biological Chemistry, 2016, 291, 16816-16827.	1.6	11
245	Co-crystallization and preliminary X-ray diffraction studies of Lathyrus ochrus isolectin I with Di- and trisaccharides, and a biantennary octosaccharide. Journal of Molecular Biology, 1990, 213, 211-213.	2.0	10
246	Combining somatic mutations present in different <i>in vivo</i> affinity-matured antibodies isolated from immunized <i>Lama glama</i> yields ultra-potent antibody therapeutics. Protein Engineering, Design and Selection, 2016, 29, 123-133.	1.0	10
247	Surfactant Poloxamer 188 as a New Crystallizing Agent for Urate Oxidase. Crystal Growth and Design, 2009, 9, 4199-4206.	1.4	9
248	Wine Phenolic Compounds Differently Affect the Host-Killing Activity of Two Lytic Bacteriophages Infecting the Lactic Acid Bacterium Oenococcus oeni. Viruses, 2020, 12, 1316.	1.5	9
249	Crystallization and preliminary X-ray studies of two isolectins from the seeds of Lathyrus ochrus. Journal of Molecular Biology, 1988, 202, 685-687.	2.0	8
250	Crystallization and Preliminary X-ray Analysis of a New Crystal form of Nitrite Reductase from Pseudomonas aeruginosa. Journal of Molecular Biology, 1994, 243, 347-350.	2.0	8
251	Structure Prediction and Analysis of Hepatitis E Virus Non-Structural Proteins from the Replication and Transcription Machinery by AlphaFold2. Viruses, 2022, 14, 1537.	1.5	8
252	Structure-function relationships of pancreatic lipases. Lipid - Fett, 1998, 100, 96-102.	0.6	7

#	Article	IF	CITATIONS
253	Insight into odorant perception: the crystal structure and binding characteristics of antibody fragments directed against the musk odorant traseolide. Journal of Molecular Biology, 1999, 292, 855-869.	2.0	7
254	Crystal structure of E. coli yddE protein reveals a striking homology with diaminopimelate epimerase. Proteins: Structure, Function and Bioinformatics, 2004, 55, 764-767.	1.5	7
255	The crystal structure of ORF14 from <i>Sulfolobus islandicus</i> filamentous virus. Proteins: Structure, Function and Bioinformatics, 2009, 76, 1020-1022.	1.5	7
256	Crystal structure of AFV1â€102, a protein from the acidianus filamentous virus 1. Protein Science, 2009, 18, 845-849.	3.1	7
257	Structural Insights into Lactococcal Siphophage p2 Baseplate Activation Mechanism. Viruses, 2020, 12, 878.	1.5	7
258	The Odorant-Binding Proteins of the Spider Mite Tetranychus urticae. International Journal of Molecular Sciences, 2021, 22, 6828.	1.8	7
259	Anchoring the T6SS to the cell wall: Crystal structure of the peptidoglycan binding domain of the TagL accessory protein. PLoS ONE, 2021, 16, e0254232.	1.1	7
260	Crystal Structure of ATVORF273, a New Fold for a Thermo- and Acido-Stable Protein from the Acidianus Two-Tailed Virus. PLoS ONE, 2012, 7, e45847.	1.1	7
261	Crystallization and preliminary X-ray analysis of the C-terminal fragment of PorM, a subunit of thePorphyromonas gingivalistype IX secretion system. Acta Crystallographica Section F, Structural Biology Communications, 2015, 71, 71-74.	0.4	6
262	Production, crystallization and X-ray diffraction analysis of a complex between a fragment of the TssM T6SS protein and a camelid nanobody. Acta Crystallographica Section F, Structural Biology Communications, 2015, 71, 266-271.	0.4	6
263	Structure–Function Analysis of the C-Terminal Domain of the Type VI Secretion TssB Tail Sheath Subunit. Journal of Molecular Biology, 2018, 430, 297-309.	2.0	6
264	Biogenesis of a Bacteriophage Long Non-Contractile Tail. Journal of Molecular Biology, 2021, 433, 167112.	2.0	6
265	Crystallization and preliminary X-ray study of subunit III of the bovine pancreatic procarboxypeptidase A-S6 ternary complex. Journal of Molecular Biology, 1986, 189, 709-710.	2.0	5
266	Crystallization and preliminary crystallographic study of a pheromone-binding protein from the cockroachLeucophaea maderae. Acta Crystallographica Section D: Biological Crystallography, 2003, 59, 916-918.	2.5	4
267	Crystallization and preliminary X-ray diffraction analysis of protein 14 fromSulfolobus islandicusfilamentous virus (SIFV). Acta Crystallographica Section F: Structural Biology Communications, 2006, 62, 884-886.	0.7	4
268	A new non-classical fold of varroa odorant-binding proteins reveals a wide open internal cavity. Scientific Reports, 2021, 11, 13172.	1.6	4
269	Monoclonal antibody 117,C-11 recognizes three exposed regions on the surface of the Lathyrus ochrus isolectin I. Immunology Letters, 1991, 30, 47-51.	1.1	2
270	Structure of odorant binding proteins and chemosensory proteins determined by X-ray crystallography. Methods in Enzymology, 2020, 642, 151-167.	0.4	2

#	Article	IF	CITATIONS
271	Crystal structures of two camelid nanobodies raised against CldL, a component of the type IX secretion system from <i>Flavobacterium johnsoniae</i> . Acta Crystallographica Section F, Structural Biology Communications, 2021, 77, 171-176.	0.4	2